

Los Alamos National Laboratory is operated by the University of California for the United States Department of Energy under contract W-7405-ENG-38

LA-UR--82-833

DE82 012146

TITLE: CERENKOV RADIATORS FOR PHOTODIODES

**MASTER**

AUTHOR(S): James W. Toevs, P-14  
Carlton S. Young, P-14  
Paul A. Zagarino, EG&G/Santa Barbara  
Robert D. Seno, EG&G/Las Vegas

SUBMITTED TO: Conferen on Instrumentation for Nuclear Weapons Effects  
Defense Nuclear Agency  
Naval Surface Weapons Center  
White Oak, Silver Spring, Maryland  
March 30 - April 1, 1982



DISTRIBUTION OF THIS DOCUMENT IS UNLIMITED

By acceptance of this article the publisher recognizes that the U.S. Government retains a nonexclusive, royalty-free license to publish or reproduce the published form of this contribution or to allow others to do so for U.S. Government purposes.

The Los Alamos National Laboratory requests that the publisher identify this article as work performed under the auspices of the U.S. Department of Energy.

**Los Alamos** Los Alamos National Laboratory  
Los Alamos, New Mexico 87545

## CERENKOV RADIATORS FOR PHOTODIODES\*

### I. SUMMARY AND CONCLUSIONS

Several materials have been examined for use as Cerenkov converters in front of photodiodes in an effort to find a gamma detector system that has more sensitivity than a Compton detector but makes little sacrifice in bandwidth. Suprasil (fused silica) and UVT Lucite (acrylic) were 10-100 times more sensitive than a Compton detector and provided almost the same bandwidth. Barium fluoride provided almost 1000 times the sensitivity, but with a factor of 3 or 4 reduction in bandwidth. Relative sensitivities are strongly dependent on beam composition; the Cerenkov package is less sensitive to a pure  $\gamma$ -ray beam than to a  $\gamma$ -electron shower beam. Hence, beam composition must be considered in any application of these detectors. A search for dependence of the sensitivity on dose is in progress.

### II. OBJECTIVES

Analysis of fast radiative processes, such as those encountered in underground nuclear testing, requires detectors with response times of nanoseconds or less. The Compton detector, a basic tool in nuclear test diagnostics, is quite fast, but also relatively insensitive. In order to provide a detector with similar bandwidth but greater sensitivity, we have investigated several materials for use as Cerenkov radiators with photodiodes.

The Cerenkov process is intrinsically very fast, as time spread in the optical pulse depends simply on the geometrical effects of different Cerenkov cone angles for different wavelengths, hence on the material dispersion of the medium. For example, in a 10 cm radius

\*Work performed under the auspices of the U.S. Department of Energy.

water Cerenkov-detector, the red and blue light pulses are 5 ps apart. Practically, then, the optical pulse width from a Cerenkov converter is essentially just the light transit time in the converter.

A second advantage of the Cerenkov converter is found in applications involving large neutron backgrounds. Protons or heavier nuclei recoiling from neutron scattering do not radiate via the Cerenkov process, hence Cerenkov radiators have low neutron sensitivity.

### III. THEORETICAL BACKGROUND

As a function of frequency, the energy radiated per unit length of radiator is

$$\frac{dI(\omega)}{dx} = \frac{e^2 \omega}{c^2} \left[ 1 - \frac{1}{\beta^2 n(\omega)^2} \right]$$

where  $e$  = electron charge  
 $\omega$  = frequency ( $2\pi c/\lambda$ )  
 $c$  = velocity of light  
 $\beta$  = electron velocity/ $c$   
 $n$  = index of refraction of the medium.

This rate of energy loss is typically about 0.1% of the ionization loss for a relativistic particle.

If the medium has small dispersion over the range of wavelengths under study, the number of Cerenkov photons from a converter is

$$N = 2\pi\alpha L \left( \frac{1}{\lambda_2} - \frac{1}{\lambda_1} \right) \left( 1 - \frac{1}{\beta^2 n^2} \right)$$

where  $l$  = length of the converter,  
 $\alpha$  = fine structure constant (1/137)

and  $\lambda_1$  and  $\lambda_2$  limit the wavelength range being observed. In a converter with  $n$  near 1.5, this corresponds to about 400 Cerenkov photons/cm for a relativistic electron.

From the above formula, it is apparent that the efficiency of a material as a Cerenkov radiator is independent of  $Z$  and varies rather slowly with  $n$ . In dosimetry of a  $\gamma$  beam, however, one must also consider the efficiency of the radiator in converting primary  $\gamma$ 's into electrons and positrons from which Cerenkov radiation may be detected. The three major processes in which energetic photons are converted are photoelectric, Compton, and pair production. The cross sections for these processes vary with the atomic number of the radiator as  $Z^4$ - $Z^5$ ,  $Z$ , and  $Z^2$ , respectively. Hence, a dense, high- $Z$  radiator should be much more sensitive than a light, low- $Z$  radiator. For example, compare barium fluoride to acrylic plastic. Photons of 6 MeV or greater are converted primarily through pair production which varies as  $Z^2$ . The ratio of  $\rho Z^2$  for the two materials is about 400. A precise calculation of the relative sensitivities of materials is difficult because of the different  $Z$  dependences of  $\gamma$  interaction processes. A further complication is that, in practice, the gamma beam is accompanied by numerous electrons, produced as the beam traveled through air and other attenuators.

#### IV. EXPERIMENTAL PROCEDURE AND RESULTS

Seven 5 cm diameter vacuum photodiodes (ITT F4014) fitted with quartz or magnesium fluoride windows and with S-0 or cesium telluride photocathodes were evaluated with Cerenkov radiators of a variety of different materials. Materials tested were Lucite, UVT Lucite, Suprasil (fused quartz), magnesium fluoride, barium fluoride, and bismuth germanate. A 12 MeV end point bremsstrahlung beam from the EG&G, Inc. SBO Electron Line served as the fast radiation source. The FWHM of the Gaussian pulse was 50 ps. The geometry was "head on "

as shown in Fig. 1. Response to a DC gamma source was also compared, using the large  $^{60}\text{Co}$  source (1.17, 1.34 MeV) at FG&G, Inc., NLVO.

Table I shows time response parameters and relative sensitivities for several materials, compared to the standard Los Alamos kintertium plate Compton detector (HFK-10). Impulse and integral response for the various materials as well as for the Compton detector appear in Figs. 1-5.

TABLE I

Response and Relative Sensitivity for Several Materials.  
The HFK Compton Detector Sensitivity is Taken as  $1.6 \times 10^{-11}$  amps/R.

<u>Cerenkov Radiator</u>	<u>Detector Window</u>	<u>Photo-cathode</u>	<u>FWHM (ns)</u>	<u>10%-90% IRT* (ns)</u>	<u>Relative Peak Amplitude (Linac)</u>	<u><math>^{60}\text{Co}</math> Relative Sensitivity</u>
5/8" $\text{BaF}_2$	Quartz	S-4	0.96	2.10	1.00	1.00
1/2" Suprasil <sup>†</sup>	Quartz	S-4	0.43	0.90	0.16	0.012
5/8" $\text{MgF}_2$	Quartz	S-4	0.43	>3.0	0.21	0.106
1/2" UVT Lucite	Quartz	S-4	0.45	1.01	0.10	-
1 1/4" $\text{BGO}^{\text{O}}$	Quartz	S-4	0.61	( 3 $\mu\text{s}$ )	0.07	-
None	Quartz	S-4	0.38	0.88	0.05	0.004
5/8" $\text{BaF}_2$	$\text{MgF}_2$	CsTe	1.11	2.12	0.42	0.079
1/2" Suprasil	$\text{MgF}_2$	CsTe	0.47	1.24	0.05	0.003
5/8" $\text{MgF}_2$	$\text{MgF}_2$	CsTe	0.43	1.24	0.03	0.001
1 1/4" BGO	$\text{MgF}_2$	CsTe	0.34	0.84	0.05	-
None	$\text{MgF}_2$	CsTe	0.43	0.98	0.02	0.003
HFK-10 Compton Detector			0.34	0.51		0.001

\*Integral rise time.

†Fused silica

<sup>O</sup> $\text{Bi}_4(\text{Ge}_3\text{O}_{12})$

We believe that the discrepancy between the relative sensitivity at the Linac and that using the  $^{60}\text{Co}$  is due to two effects. The first is electron mix in the  $\gamma$  flux, a complication alluded to earlier. We would expect the  $^{60}\text{Co}$  geometry to provide a relatively pure  $\gamma$  beam, while the Linac geometry would provide a beam in which electrons and photons are relatively close to equilibrium ( $\sim 3 \gamma's/e^{\pm}$ ). Further studies with clearing magnets will be performed in an attempt to verify these assertions. The second effect is slow fluorescence, which will be discussed below. The  $^{60}\text{Co}$  experiments were DC anode current measurements; slow fluorescence therefore could not be excluded.

As the equilibrium (Linac pulse) situation represents more typically the situation we are likely to have in the field, and since we can ignore slow fluorescence contributions, we shall direct our conclusions to these results. For quartz windows and S-4 photocathodes, Suprasil and UVT Lucite are about 2 orders of magnitude more sensitive than the Compton detector and make little sacrifice in bandwidth. Barium fluoride shows 1000 times the sensitivity of the Compton detector, although bandwidth is lower by a factor of 2 or 3. The pulse shape is nicely behaved (Fig. 7a). For some measurements, such as early  $\alpha$  measurements on an underground nuclear test, the  $\text{BaF}_2$  - photodiode pair might be an excellent choice for coverage. The bandwidth is adequate for measuring the slowly changing  $\alpha$ , the detector is much more sensitive than an HFK, and it is much less sensitive to neutrons than a fluor such as NE111.

Bismuth germanate (BGO), which is  $\text{Bi}_4\text{Ge}_3\text{O}_{12}$ , has a high Z ( $Z_{\text{Bi}} = 83$ ), high density ( $7.13 \text{ g/cm}^3$ ), and large optical index (2.15?) which make it an interesting candidate for Cerenkov studies. Its disappointing yield is probably due to its high index. The Cerenkov angle in BGO is  $62.3^\circ$ , while the critical angle for total internal reflection between BGO and quartz ( $n = 1.5$ ) is  $42^\circ$ . Thus, little of the Cerenkov light can reach the photodiode. Attempts to find better coupling methods are underway.

Fluorescence was anticipated as a background problem with several of the materials. BGO is an excellent scintillator because of its high fluorescence yield. Quartz fluorescence has been used for years to observe low energy proton beams. It was our hope that by using  $MgF_2$  windows and CsTe photocathodes to improve our sensitivity in the UV and decrease our sensitivity in the visible, we might detect Cerenkov radiation more effectively than fluorescence. Indeed, with quartz windows and S-4 photocathodes, magnesium fluoride and BGO did demonstrate long fluorescence tails (Fig. 3a, 6a) while quartz (Suprasil), UVT Lucite, and barium fluoride did not (Fig. 2a, 2b, 7a, 7b). Using the  $MgF_2$  window and CsTe photocathode, the fluorescence tail was eliminated (Fig. 3b, 6b). To test in the magnesium fluoride radiator that the long tail was fluorescence, the geometry was reversed, so the beam passed through the photodiode, through the window, and into the radiator. In this geometry, Cerenkov light should be reduced, since the Cerenkov cone proceeds forward. Fluorescence, being radiated isotropically, should not be reduced. Figure 4 shows that these expected results were observed. We conclude that fluorescence can be eliminated with photocathode selection, but, as can be seen in Table I, a price is paid in sensitivity.

The specific magnesium fluoride samples under study had been irradiated for some time in earlier experiments. The total dose should have been only about 20% of the dose required to produce color centers, however, we felt that new samples should be examined. Indeed, new samples showed no evidence of slow fluorescence. Spectral examination of the DC light response revealed a large peak between 500 and 650 nm in the old (damaged)  $MgF_2$ , and no such peak in the new samples. As magnesium fluoride was not sufficiently sensitive to warrant further study, its dose dependence does not present a problem. However, it is clearly prudent to examine response linearity and shape versus radiation dose for those materials that will have practical application. Such studies will be carried out in the near future.

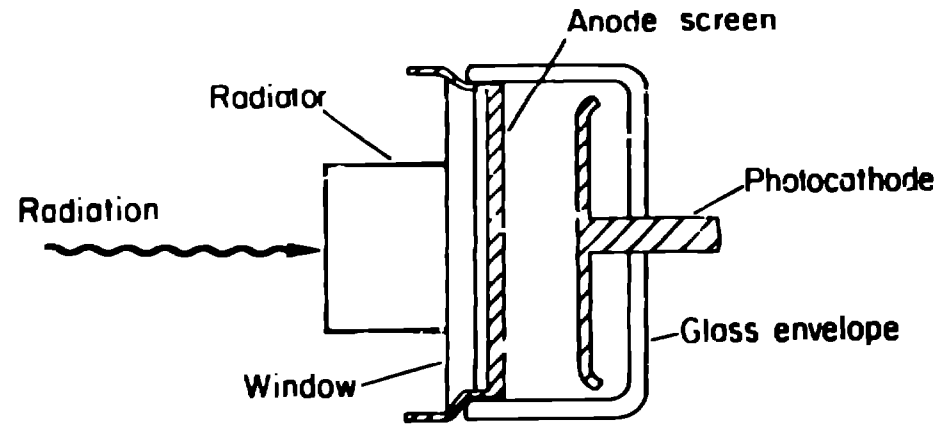


Fig. 1. Experimental Geometry

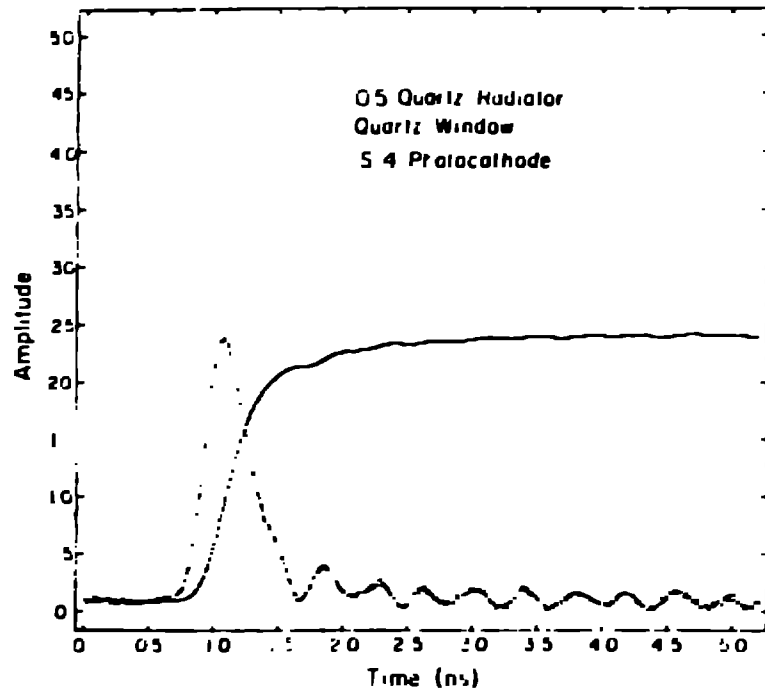


Fig. 2a.

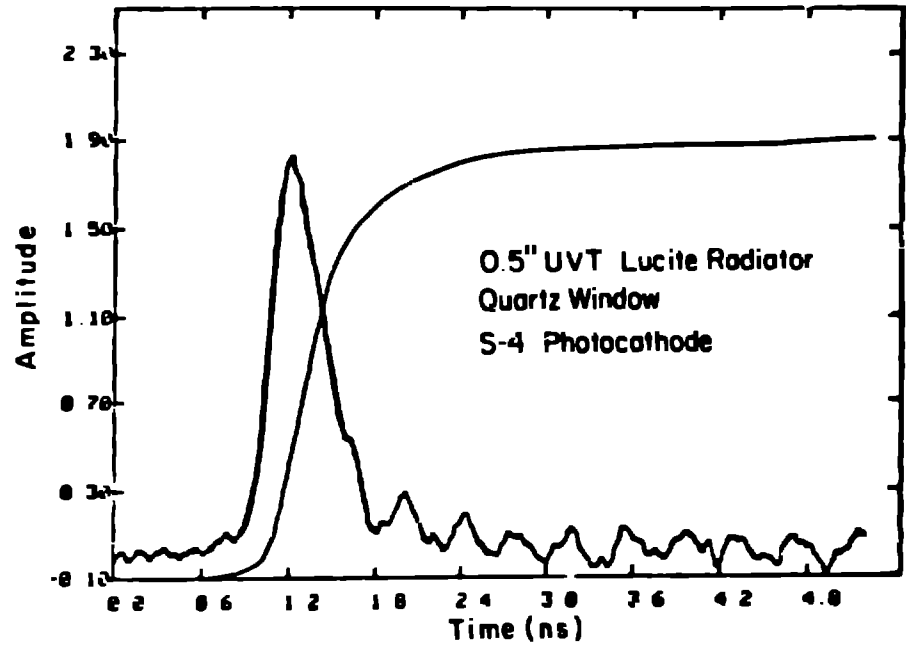


Fig. 2b.

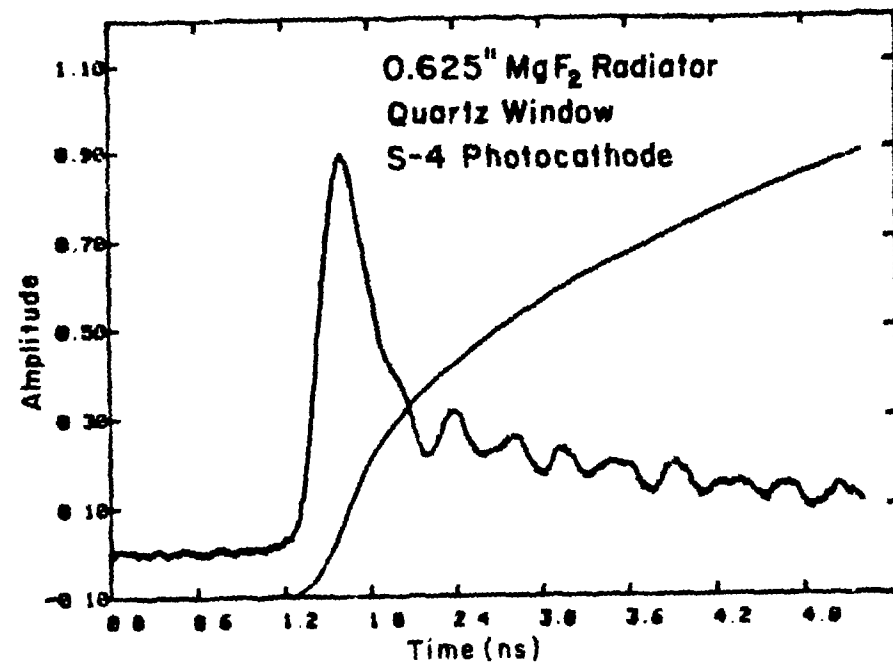


Fig. 2a.

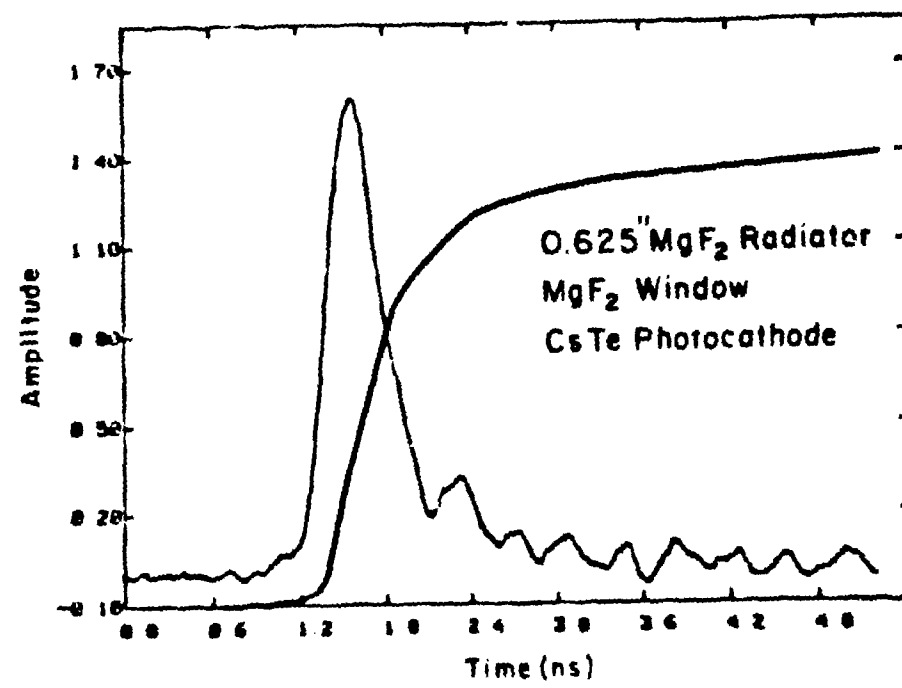


Fig. 3b.

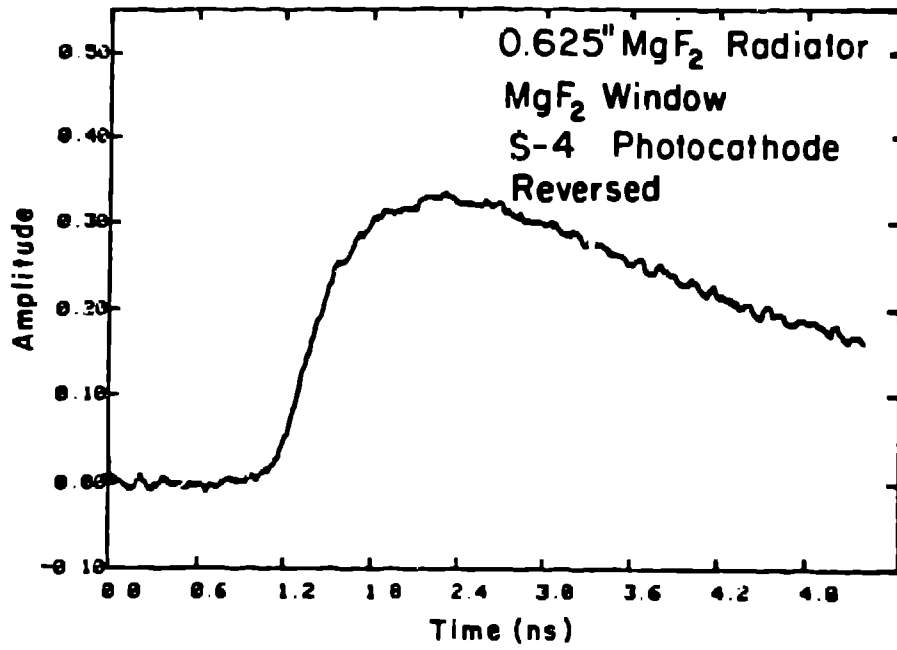


Fig. 4.

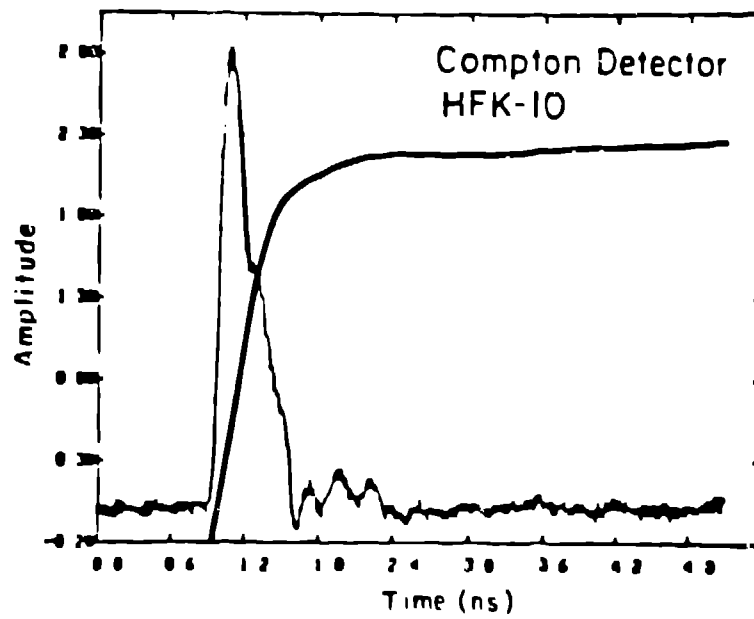


Fig. 5.

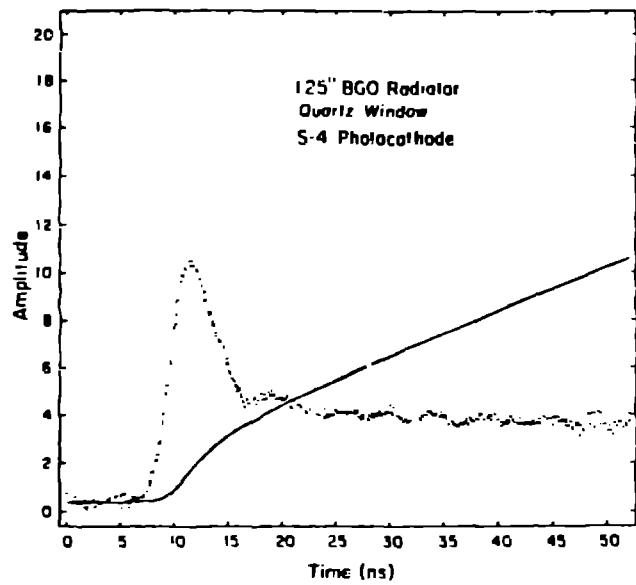


Fig. 6a.

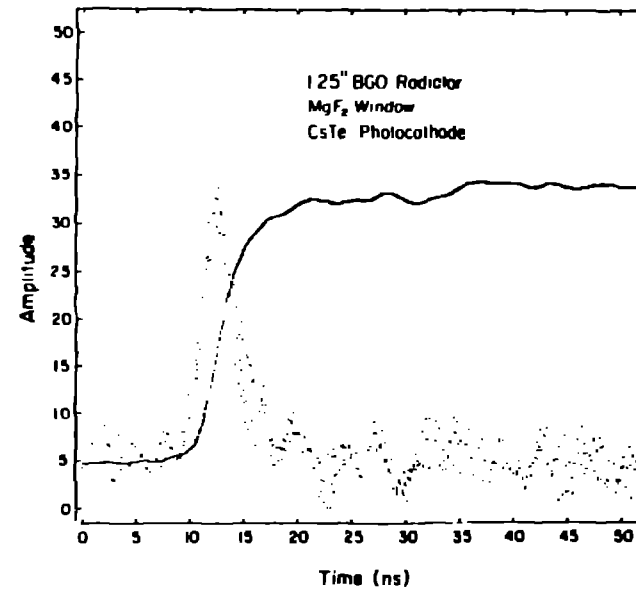


Fig. 6b.

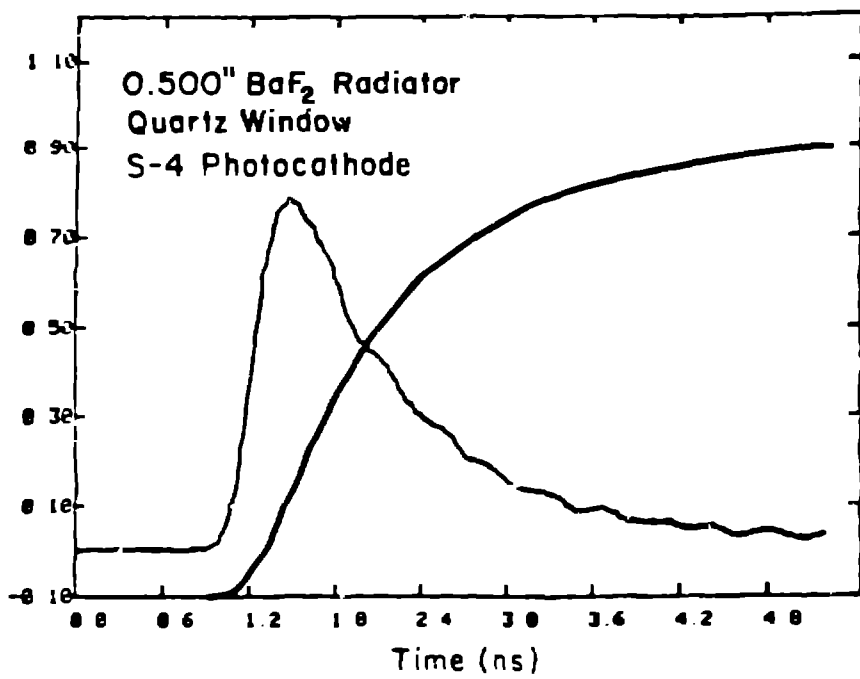


Fig. 7a.

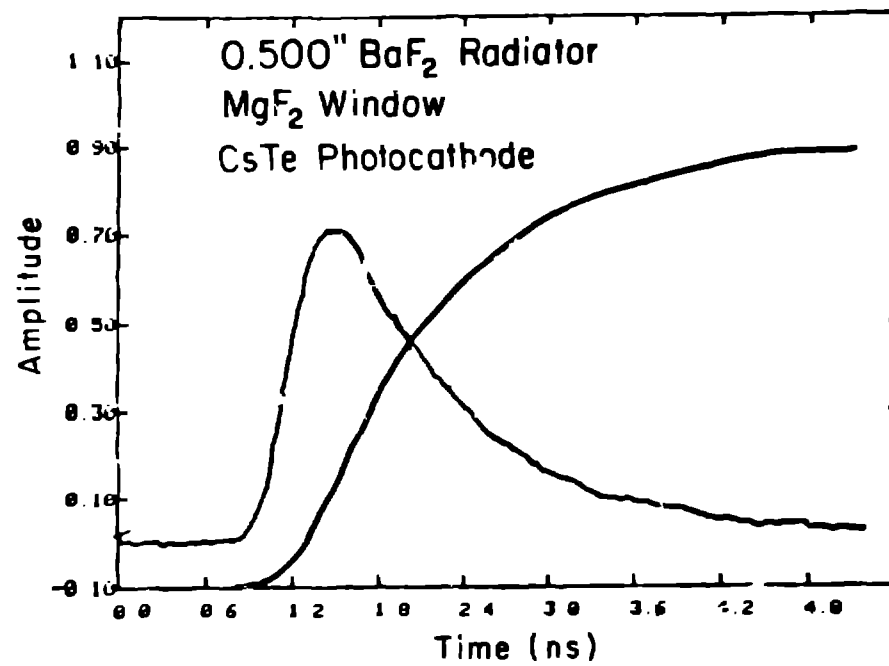


Fig. 7b.